

POLARIZED PROTON AND ANTIPOTON EXPERIMENTS  
AT FERMILAB E-581/704

ANL-HEP-CP--88-78

DE89 005869

JAN 20 1989

A. Yokosawa  
Argonne National Laboratory Argonne, IL 60439  
(For the E-704 Collaboration)

### ABSTRACT

We summarize activities concerning the Fermilab polarized beams. They include a description of the polarized-beam facility, measurements of beam polarization by polarimeters, asymmetry measurements in the  $\pi^0$  production at large  $x$ , and experiments with polarized beams during the next fixed-target period.

### INTRODUCTION

The Fermilab polarized-beam program designated as E-581/704 initiated and carried out by an international collaboration, Argonne (U.S.), Fermilab (U.S.), Univ. of Iowa (U.S.), Kyoto Univ. (Japan), Kyoto Sangyo Univ. (Japan), Kyoto Univ. of Education (Japan), Hiroshima Univ. (Japan), Univ. of Occup. and Environ. Health (Japan), LAPP-Annecy (France), Northwestern University (U.S.), Los Alamos Laboratory (U.S.), Rice (U.S.), CEN-Saclay (France), IHEP-Serpukhov (U.S.S.R.), INFN-Trieste (Italy)

The physics objectives for the Fermilab polarized-beam facility up to 200 GeV/c are in part based upon the facts that there are already several experimental indications that spin effects are significant at high energy. They are i) measurements of  $\pi^0$  production at high  $p_T$  ( $p_T > 2.0$  GeV/c) in proton-proton at CERN and in  $\pi^-$ -proton collisions at Serpukhov revealed sizeable asymmetries at 24 GeV/c and 40 GeV/c, respectively ii) hyperons produced at large  $x_F$  inclusively off nuclei and hydrogen at CERN, Fermilab, and ISR were observed to have high polarizations iii) inelastic scattering of longitudinally polarized electrons on longitudinally polarized protons at SLAC yielded a large asymmetry, implying that proton helicity orientation is communicated to the constituent quarks iv) results of new EMC measurements have interpreted that the proton spin may not be due to the helicity of its constituent quarks. Most of the proton spin may be due to gluons and/or orbital angular momentum. To understand the basic question of the proton spin, hadron-production measurements at high  $p_T$  with longitudinally polarized protons on longitudinally polarized target protons seem to be very desirable.

MASTER

## POLARIZED-BEAM FACILITY

The polarized-beam facility was operated during the last TeV-II (fixed target) period which ended 15 February 1988.

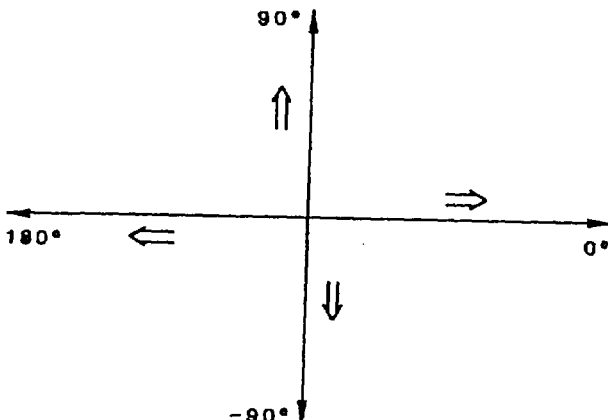
An extracted beam from the Tevatron is delivered through the MP primary-beam line to the Meson Detector Building where a 0.73 interaction length Be target is utilized to produce  $\Lambda^0$  and  $\bar{\Lambda}^0$  at  $\theta_{c.m.} \approx 0^\circ$ . Protons and antiprotons from the  $\Lambda^0$  and  $\bar{\Lambda}^0$  decays respectively are brought to a final target position in the MP hall through the MP secondary beam (200 GeV/c) line.

The polarization comes from the parity violating decays of  $\Lambda^0$ 's ( $\bar{\Lambda}^0$ 's). The protons (antiprotons) from the  $\Lambda^0 + p\pi^-$  ( $\bar{\Lambda}^0 + \bar{p}\pi^+$ ) decay have a polarization of 64% along the direction in the  $\Lambda_{c.m.}$  ( $\bar{\Lambda}_{c.m.}$ ) and the  $\Lambda^0$  ( $\bar{\Lambda}^0$ ) decay is isotropic. We use  $\Lambda^0$ 's ( $\bar{\Lambda}^0$ 's) produced at the low  $p_T$  where the production cross section is maximum and the  $\Lambda^0$ 's ( $\bar{\Lambda}^0$ 's) are unpolarized.

The spin direction in the lambda center-of-mass (decay frame) is shown in Fig. 1. We note that spin direction is almost unchanged in transforming from the lambda-decay frame to the laboratory. Therefore protons or antiprotons decaying around  $\theta_{c.m.} = 0^\circ$  and  $180^\circ$  are longitudinally polarized ( $\hat{L}$ ) while those with  $\theta_{c.m.} = \pm 90^\circ$  are transversely polarized ( $\hat{N}$ , up and down, or  $\hat{S} = \hat{N} \times \hat{L}$ ) in the laboratory.

Fig. 1

Spin direction of protons vs. decay angles. The spin direction is indicated by  $\Rightarrow$  and  $\downarrow$  symbols.



For a beam line with the "longitudinal mode", one could select high-momentum protons which are forward decaying, around  $\theta_{c.m.} = 0^\circ$ , from lambdas near the highest energy portion of the  $\Lambda^0$  production spectrum. For a beam line with the "transverse mode", it has been shown that we can select protons or antiprotons at various momenta which are decaying around  $\theta_{c.m.} = 90^\circ$  from lambdas or antilambdas respectively. We show how this scheme works.

Protons or antiprotons with  $\theta_{c.m.} = 90^\circ$  and  $-90^\circ$  have the opposite laboratory decay angles which are not zero. They can be distinguished from those decaying at  $\theta_{c.m.} = 0^\circ$  from lambda or antilambda with the production target as the source of the beam. Virtual sources for  $|\theta_{c.m.}| = 90^\circ$  particles are illustrated in Fig. 2. The spin direction,  $N$  or  $S$ , should be chosen using the field direction of the sweeping magnets and bending magnets for the momentum selection, so that the spin direction is parallel to the field.

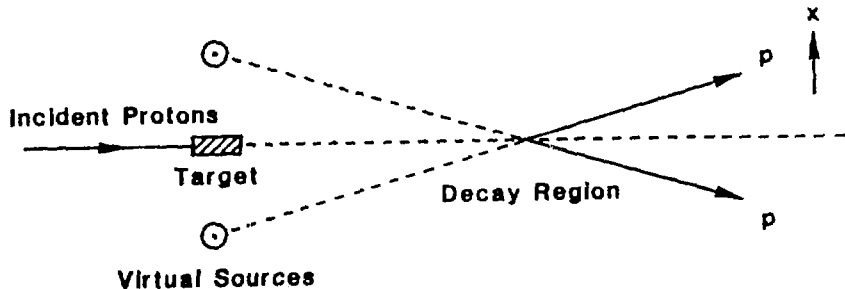


Fig. 2 Virtual sources (top view).

The secondary beam line up to 200 GeV/c is shown in Fig. 3. Here the field direction is in the  $x$  direction and the spin direction is in the  $S$  direction.

Polarized protons from the virtual sources as shown in Fig. 2 are focussed in the tagging section, where both the momentum and polarization are selected (see Fig. 3).<sup>1</sup> The polarization is

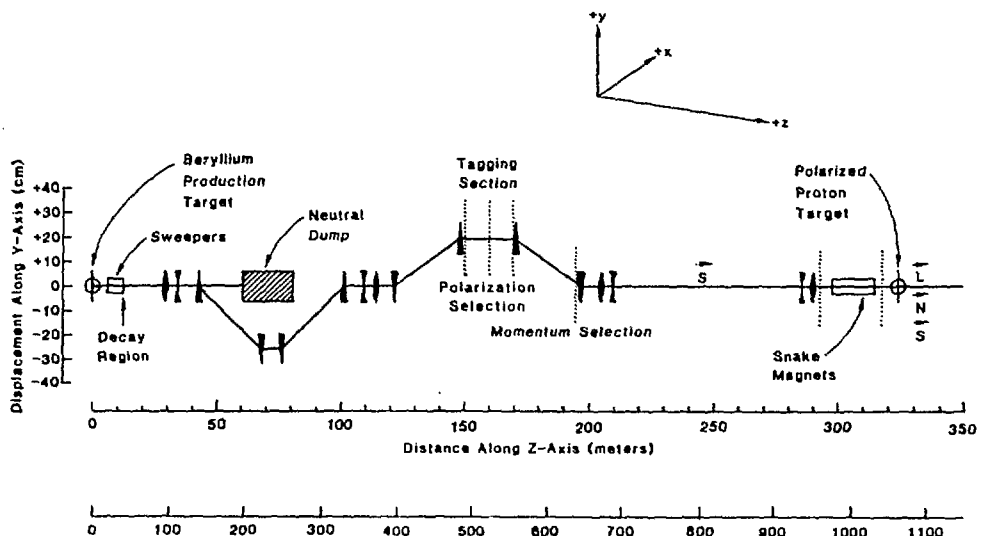


Fig. 3 Side view of the Fermilab polarized beam (MP secondary beam).

strongly related to the x position ( $x$ ,  $y$ ,  $z$  directions are indicated in Fig. 3) at the tagging section, and the average polarization,  $\langle P \rangle$ , and  $I\langle P \rangle^2$ , where  $I$  represents actually measured beam intensity, are shown in Figs. 4 and 5 respectively with respect to  $x$  in mm.

Then the  $\vec{S}$  type beam reaches the snake magnets which make fast reversal, typically every 10 spills, of the spin direction. The snake magnets consisting of twelve dipoles with  $45^\circ$  precessions as shown in Fig. 6 can also change the spin direction from  $\vec{S}$  to  $\vec{N}$  or  $\vec{S}$  to  $\vec{L}$  without altering beam direction and phase space before and after the magnets. These magnets are expected to control systematic errors by periodic reversal.

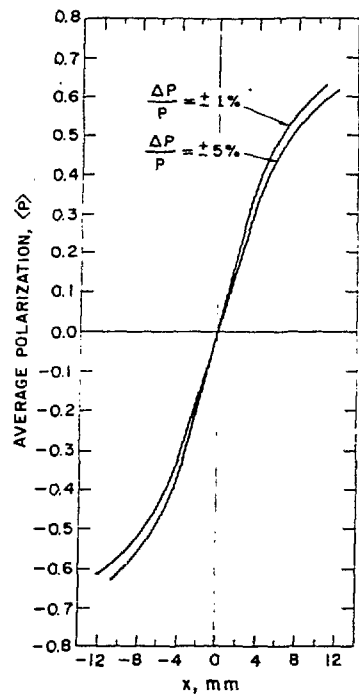


Fig. 4  $\langle P \rangle$  vs.  $x$  in the tagging section.

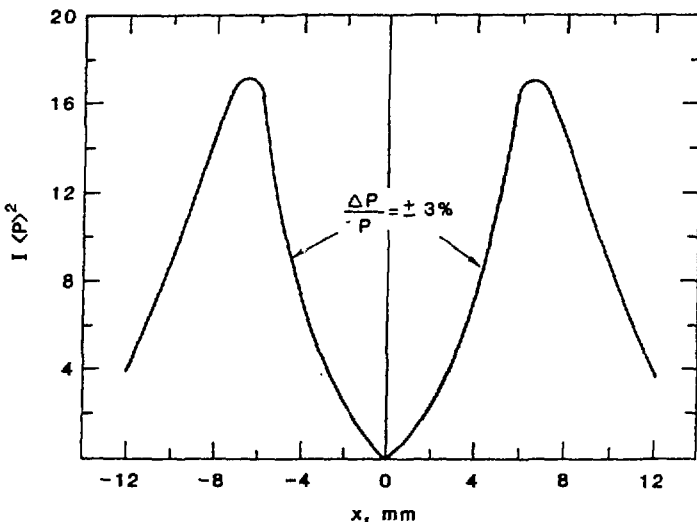


Fig. 5  $\langle P \rangle^2$  (arbitrary unit) vs.  $x$  in the tagging section.

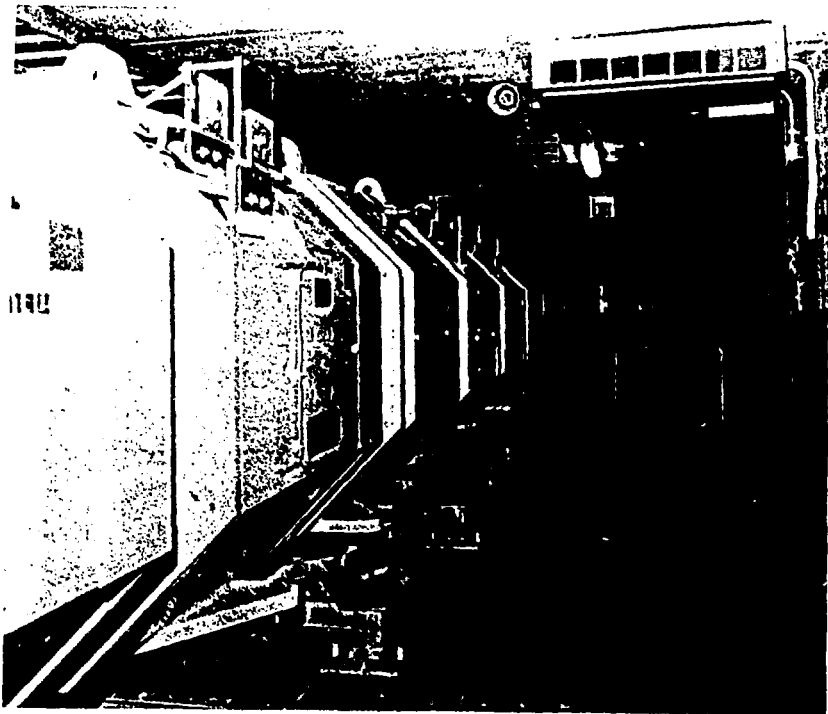


Fig. 6 Photograph of the snake magnets consisting of 12 dipoles located at the entrance to the experimental hall.

#### INITIAL OPERATION OF THE POLARIZED BEAM

During the recent fixed-target run at Fermilab, this beam line was initially commissioned with 30-GeV hadrons and positrons for beam-line tuning and calibration of various detectors. Several weeks were provided with 800-GeV protons incident on the beryllium target, in order to study the proton and antiproton yields and to measure the beam polarization. Usable protons and antiprotons were selected by their tagged position corresponding to a calculated polarization magnitude of  $> 35\%$  equivalent to the average polarization of 45%. Two threshold Cerenkov counters were used upstream of the snake magnets to reject pions in the beam. Measurements of the beam flux for  $1 \times 10^{12}$  incident protons per 20-sec spill were:

---

	Tagged Beam ( $P_{av} = 45\%$ )	Total Protons (antiprotons)	Background $\pi$ 's
Protons	$8 \times 10^6$	$1.5 \times 10^7$	$1.5 \times 10^6$
Antiprotons	$4 \times 10^5$	$7.5 \times 10^5$	$3.8 \times 10^6$

---

These measured intensities are in good agreement with design calculations. An increase in the primary intensity to  $4 \times 10^{12}$  incident protons/20-sec spill is expected for the next data-taking period and then the beam flux will be:

	Tagged Beam ( $P_{av} = 45\%$ )	Total Protons (antiprotons)	Background $\pi$ 's
Protons	$3.2 \times 10^7$	$6 \times 10^7$	$6 \times 10^6$
Antiprotons	$1.6 \times 10^6$	$3 \times 10^6$	$1.5 \times 10^7$

Detectors in the MP experimental hall including beam hodoscopes, transmission hodoscopes, multiwire proportional chambers, lead-glass calorimeters, etc. are shown in Fig. 7.

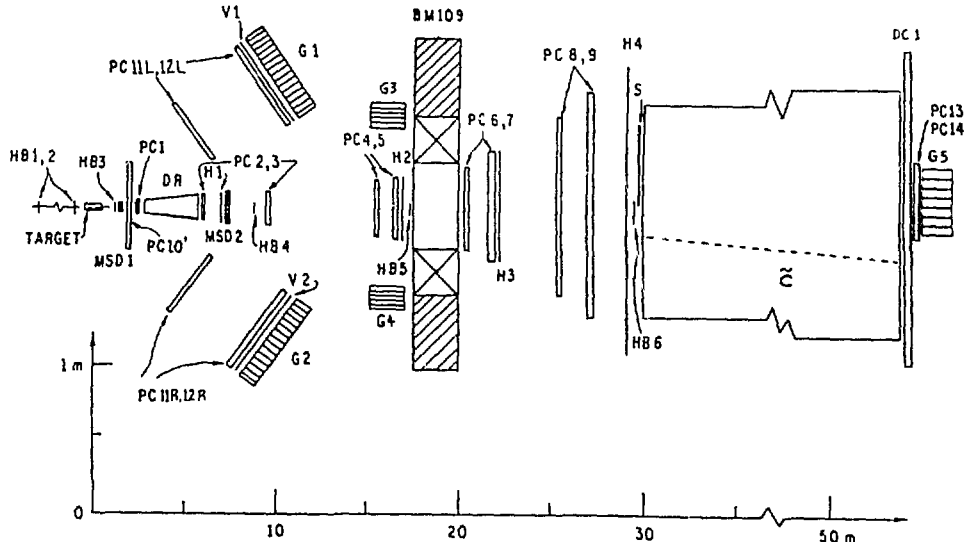


Fig. 7 Detectors in the MP experimental hall (top view).  
HB1,2,3,: beam hodoscope, HB4,5,6: transmission hodoscope,  
Target: polarized proton target/hydrogen target/polarimeter target,  
H1 to H4: trigger hodoscope, MSD1,2: multistrip solid-state  
detector, PC1 to 14: MWPC, V1, V2: veto hodoscope, G1,2: lead-  
glass calorimeter, G3,4: lead-glass hodoscope.

Two polarimeters were used to measure the absolute polarization and to confirm the validity of the tagging method. We describe the function of these polarimeters in the experimental hall.

### PRIMAKOFF-EFFECT POLARIMETER

This polarimeter relies on the Primakoff effect, where the analyzing power for dissociation of an incoming high-energy proton into a ( $\pi N$ ) system by the Coulomb field of a heavy nucleus can be related to the known low-energy polarized-target asymmetry in photoproduction of the corresponding ( $\pi N$ ) system (see Fig. 8). Asymmetries in the low-energy photoproduction are quite large, up to 90% in certain kinematic regions. The same analyzing power in the corresponding kinematic region will occur in the proton-induced process at high energy. Using a 3-mm lead target, lead-glass calorimeter, and a magnetic spectrometer, it was possible to observe the Primakoff events in the  $|t| < 10^{-3} (\text{GeV}/c)^2$  region and the mass range,  $1.34 < M(p, \pi^0) < 1.50 \text{ GeV}$ . About 3000 events using protons with tagged average polarizations of 45% were collected in 48 hours. The beam polarization was determined to be  $(40 \pm 10)\%$ , in agreement with the design calculations.<sup>2</sup> No asymmetries were found in kinematic regions where the low-energy photoproduction data show a zero analyzing power. Data collected in a short run with the polarized-antiproton beam were only sufficient to observe the Primakoff process.

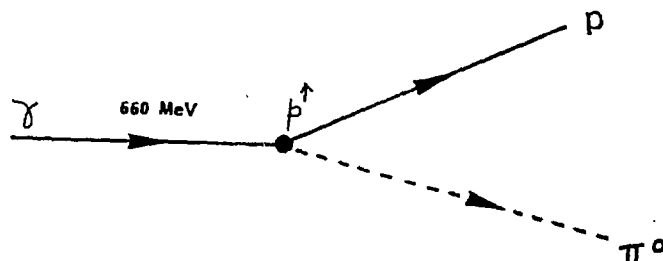
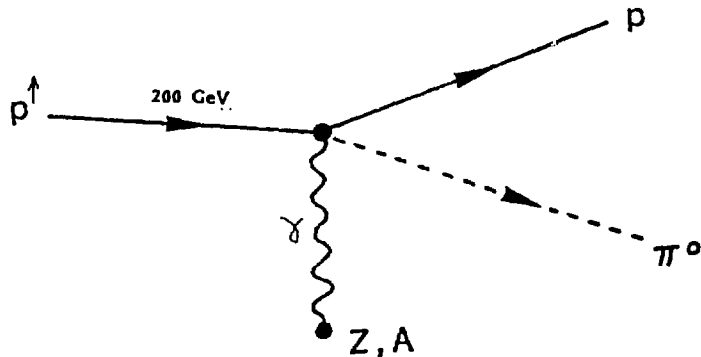


Fig. 8 Primakoff effect.

### COULOMB-NUCLEAR POLARIMETER (CNI)

The CNI polarimeter uses the Coulomb-nuclear interference effect in  $p\bar{p}$  ( $p\bar{p}$ ) elastic scattering.<sup>3</sup> The analyzing power, arising from the interference term between the nuclear non-flip amplitude and the electromagnetic spin-flip amplitude, is  $\sim 5\%$  at  $|t| = 3 \times 10^{-3}$   $(\text{GeV}/c)^2$  and is energy independent. We utilized a scintillator target to detect the recoil proton and a forward spectrometer to detect the scattered proton. A one-day measurement was sufficient to show that elastic scattering from hydrogen in the active scintillator target could be distinguished from background. The beam polarization was determined to be  $(41 \pm 25)\%$  which should be compared with the value of 42% obtained from tagging.

We also obtained uncorrelated events (without detecting the recoil proton) at low  $|t| < 3 \times 10^{-3}$   $(\text{GeV}/c)^2$ . Although further studies are needed, they are likely due to elastic scattering from carbon or from hydrogen with relatively small contributions from inelastic processes such as diffractive dissociation or quasi-free scattering. The corresponding analyzing power should be only slightly diluted with respect to that from  $p\bar{p}$  elastic scattering. By assuming the latter analyzing power, the beam polarization was determined to be  $(22 \pm 8)\%$  for protons with tagged average polarization of 42%.

We performed the same analysis for uncorrelated antiproton events. The antiproton beam polarization was determined to be  $(42 \pm 17)\%$  compared with the tagged polarization of 42%.

### ASYMMETRY MEASUREMENTS IN THE $\pi^0$ PRODUCTION

Using the new 185-GeV/c polarized proton and antiproton beams, asymmetry measurements in  $\pi^0$  production at large  $x$  were carried out.<sup>4</sup>

$p^+ (N) + (\text{hydrocarbon}) \rightarrow \pi^0 + X$   
at  $0.28 < x_F < 0.73$ ,  $0.41 < p_{\perp} < 1.02 \text{ GeV}/c$

$\bar{p}^+ (N) + (\text{hydrocarbon}) \rightarrow \pi^0 + X$   
at  $\langle x_F \rangle = 0.38$  and  $\langle p_{\perp} \rangle = 0.6 \text{ GeV}/c$

The detector consisted of an electromagnetic calorimeter with two sequential sections of 124 lead-glass modules ( $6.35 \times 6.35 \text{ cm}^2$ ,  $12 X_0$ ) and a lead-scintillation sandwich ( $\sim 20 X_0$ ).

The asymmetry in  $\pi^0$  production was determined by measuring the difference between the number of events with spin up and down beams divided by the sum; that is

$$A = (1/P_B) \{N((\uparrow) - N(\downarrow)\}/\{N(\uparrow) + N(\downarrow)\},$$

where  $P_B = 0.40$ .

The average values measured for protons were  $0.10 \pm 0.03$  and for antiprotons  $-(0.26 \pm 0.19)$ .

Our results encourage us to extend these measurements to other mesons and hyperons to provide a more complete picture of the mechanism involved in these processes yielding the significant asymmetry.

#### POLARIZED-BEAM EXPERIMENTS DURING NEXT FIXED-TARGET RUN

Experiment 704, the Integrated Proposal on First Round Experiments with the Polarized Beam Facility, constitutes a proposal to simultaneously perform substantial parts of previously proposed Experiments # 674 (Asymmetries in Inclusive Pion and Kaon Production at Large  $x$  with a Polarized Beam), # 676 (An Experiment to Measure  $\Delta\sigma_L$  in  $p$ - $p$  and  $\bar{p}$ - $p$  Scattering Between 100 and 500 GeV), # 677 (To Study the Spin Dependence in the Inclusive Production of Lambda Particles with the Polarized Beam), and # 678 (Proposal to Study the Spin Effects in Inclusive  $\pi^0$  and Direct Gamma Production at High- $p_T$  with the Polarized Beam Facility).

A)  $\Delta\sigma_L(p\bar{p})$  and  $\Delta\sigma_L(\bar{p}p)$

We intend to explore the spin dependence of the interactions in a global way using a straightforward experiment which will measure the difference in  $p\bar{p}$  and  $\bar{p}p$  total cross sections between the states with helicities of target and beam parallel and antiparallel.

$$\Delta\sigma^{\text{Tot}} = \sigma^{\text{Tot}}(\uparrow) - \sigma^{\text{Tot}}(\downarrow).$$

Experience shows that accuracy of  $\pm 100$  microbarns can easily be achieved.

In  $\bar{p}p$  interactions there are also good reasons to expect polarization effects at the highest energies. In any process at relativistic energy involving the annihilation of spin-1/2 particles into vector intermediate states, a reaction with initial particles having like helicities is almost completely suppressed (by a factor  $\gamma$ ) relative to the rate for the same reaction in a state of opposite helicities.

B) Hadron production on hydrogen target with polarized beam,  
 $p \uparrow p \rightarrow (\pi^0, \pi^\pm, \Lambda^0, \Sigma^0) + X$

We will simultaneously study the inclusive production of neutral pions around  $x_F \approx 0$  at large  $p_T$ , and of  $\Lambda^0, \Sigma^0$  at large  $x$ . We will measure single-spin asymmetries in the hadron production,

$$A_N = (E \cdot d^3\sigma/dp^3 \uparrow - E \cdot d^3\sigma/dp^3 \downarrow) / (E \cdot d^3\sigma/dp^3 \uparrow + E \cdot d^3\sigma/dp^3 \downarrow),$$

where the arrows refer to the transversity of the incoming proton. Interpretation of the polarization of hyperons ( $\Lambda, \Sigma, \Xi$ ) produced inclusively ( $pp \rightarrow \Lambda^0 \uparrow X, Kp \rightarrow \Lambda^0 \uparrow X$ , etc.) has given rise to extensive discussion about the origin of this polarization. We expect that information of spin transfer from initial to final state in this reaction will enlighten the debate.

The major detectors for this experiment are: i) two gamma spectrometers (called CEMC, central electromagnetic calorimeter), G1 and G2 as shown in Fig. 7, with 500 lead-glass cells each will be used to detect  $\gamma$ 's from  $\pi^0$  decay. Figure 9 shows the photograph of the CEMC in the experimental hall. ii) The magnetic spectrometer with proportional and drift-chamber systems (PC's and DC1 as shown in Fig. 7) and with a Cerenkov counter followed by lead-glass cells is to detect  $\pi^\pm, \Lambda^0$ , and  $\Sigma^0$ .

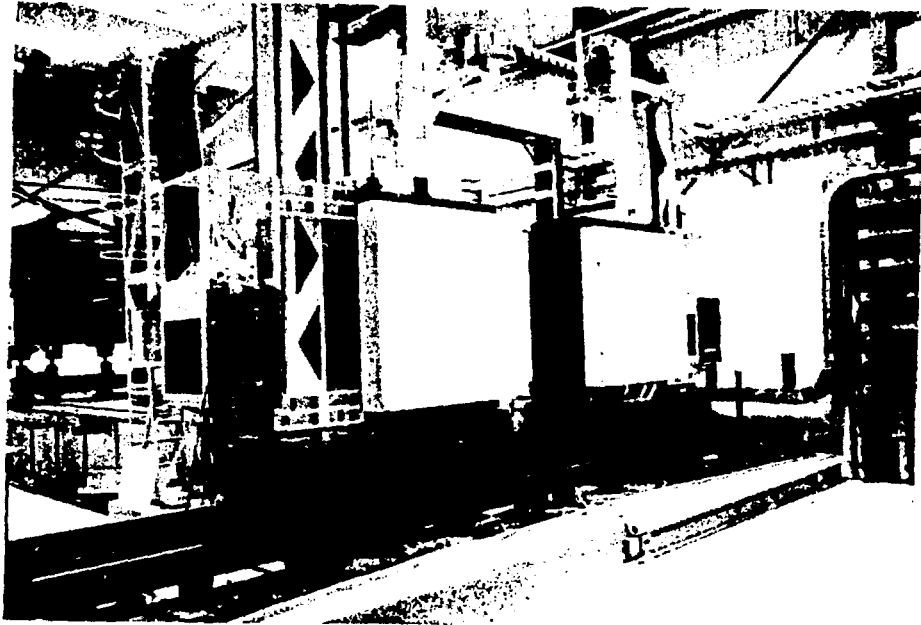
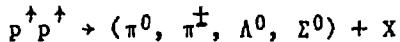


Fig. 9 Photograph of the CEMC (Central Electromagnetic Calorimeter).

## SECOND ROUND EXPERIMENTS

During the first-round hadron production experiments, we will study the one-spin effect as mentioned above. As obvious follow-up experiment we would measure the hadron production using the Polarized-Beam Facility and the Polarized Target Facility. We will measure the difference between the hadron production cross sections for helicities of beam and target parallel and antiparallel.



While a perturbative QCD seems to have problems in predicting the polarization in the hadron production, it has a definite prediction for the hadron production at high  $p_\perp$  in the pure helicity states.

## FUTURE EXPERIMENTS

Thus far, we have discussed large- $p_\perp$   $\pi^0$  and large- $X$  hadron production measurements with polarized beams, since these channels are relatively easier to make measurements. We also would like to explore large- $p_\perp$   $\pi^\pm$ , direct gamma production, and calorimeter triggered events.

Interpreting the new EMC results, Brodsky, Ellis, and Karliner<sup>5</sup> suggested that most of the proton spin is due to gluons and/or orbital angular momentum and discussed various measurements to test this suggestion. Some of the experiments can be carried out with the Fermilab polarized beams. Direct experimental information on the gluon polarization in a proton may be obtained in the measurements of  $p^\uparrow p^\uparrow \rightarrow$  (Hadronic Jet or Direct photon)  $X$  at large  $p_\perp$  and  $p^\uparrow p^\uparrow \rightarrow$  (hyperon)  $X$  at large  $p_\perp$ .<sup>6-7</sup> The interesting problem of how the spin of a hadron is shared among constituents may be tested in the proton-proton Drell-Yan process with polarized beam and target,  $p^\uparrow p^\uparrow \rightarrow (\ell^+ \ell^-) X$ .<sup>8</sup>

Pending proposals using the Fermilab polarized-beam facility at the moment are proposed experiments #682 (Study of the  $p_\perp$  Dependence of  $\pi^\pm$  Inclusive Production with a Polarized Proton Beam and Target), #688 (Nuclear-Size Dependence of Single-Spin Asymmetries in High- $p_\perp$  Hadron Production), and #699 (Study of Spin-Dependent Asymmetries Using Calorimeter Triggered High- $p_\perp$  Events with Polarized Beam and Polarized Target).

<sup>†</sup> Work supported in part by the U.S. Department of Energy,  
Division of High Energy Physics, Contract W-31-109-ENG-38.

**REFERENCES**

**\* The E-581/704 Collaboration:**

N. Arkchurin, D. Carey, R. Coleman, D. Cossairt,  
A. Derevschikov, D. P. Grosnick, M. M. Gazzaly, D. Hill,  
K. Imai, M. Laghai, F. Lehar, A. deLesquen, D. Lopiano,  
F. C. Luehring, K. Kuroda, A. Maki, A. Masaike,  
Yu. A. Matulenko, A. P. Meschanin, A. Michalowicz,  
D. H. Miller, K. Miyake, T. Nagamine, F. Nessi-Tedaldi,  
M. Nessi, S. B. Nurushev, Y. Ohashi, Y. Onel, G. Pauletta,  
A. Penzo, G. C. Phillips, A. L. Read, J. B. Roberts,  
L. vanRossum, G. Salvato, P. Schiavon, T. Shima,  
V. L. Solovyanov, H. Spinka, R. W. Stanek, R. Takashima,  
F. Takeuchi, N. Tanaka, D. G. Underwood, A. N. Vasilev,  
A. Villari, A. Yokosawa, T. Yoshida, A. Zanetti.

1. F. Luehring, Hadron Beams Session in this Symposium.
2. T. Yoshida, Polarimeters Session in this Symposium.
3. G. Pauletta, Polarimeters Session in this Symposium.
4. F. Nessi-Tedaldi, High Energy Hadron Interactions  
(fragmentation) Session in this Symposium; B. E. Bonner et al.,  
Phys. Rev. Lett. 61, 1918 (1988).
5. S. J. Brodsky, J. Ellis, and M. Karliner, Phys. Lett. 206, 309  
(1988).
6. M. B. Einhorn and J. Soffer, Nucl. Phys. 274, 714 (1986).
7. N. S. Craigie, V. Roberto, and D. Whould, Zeit. Phys. C12, 173  
(1982).
8. E. Richter-Wgs and J. Szwed, Phys. Rev. D31, 633 (1985).

## **DISCLAIMER**

This report was prepared as an account of work sponsored by an agency of the United States Government. Neither the United States Government nor any agency thereof, nor any of their employees, makes any warranty, express or implied, or assumes any legal liability or responsibility for the accuracy, completeness, or usefulness of any information, apparatus, product, or process disclosed, or represents that its use would not infringe privately owned rights. Reference herein to any specific commercial product, process, or service by trade name, trademark, manufacturer, or otherwise does not necessarily constitute or imply its endorsement, recommendation, or favoring by the United States Government or any agency thereof. The views and opinions of authors expressed herein do not necessarily state or reflect those of the United States Government or any agency thereof.